

Original Article

Open Access



Real-time *in vivo* structure-function study of scalp hair cycles: an experimental approach for monitoring living hair roots with a 20-year follow-up

Dominique Van Neste

Skin and Hair Clinic, Skinterface, Brussels B-1200, Belgium.

Correspondence to: Dr. Dominique Van Neste, Skin and Hair Clinic, Skinterface, 121 avenue du Couronnement, Brussels B-1200, Belgium. E-mail: info@skinterface.be

How to cite this article: Van Neste D. Real-time *in vivo* structure-function study of scalp hair cycles: an experimental approach for monitoring living hair roots with a 20-year follow-up. *Plast Aesthet Res.* 2025;12:4. <https://dx.doi.org/10.20517/2347-9264.2024.114>

Received: 24 Aug 2024 **First Decision:** 11 Nov 2024 **Revised:** 14 Feb 2025 **Accepted:** 17 Feb 2025 **Published:** 28 Feb 2025

Academic Editor: Mark K. Wax **Copy Editor:** Ting-Ting Hu **Production Editor:** Ting-Ting Hu

Abstract

Aim: This study presents an experimental approach for the long-term (16 years) *in vivo* observation of deeper structures in human scalp hair follicles, focusing on shortened hair cycles. When hair follicles entered a prolonged dormancy stage (3 years), rapid regrowth of thinning hair was stimulated by the topical application of a drug approved for promoting hair growth.

Methods: While intra-epidermal chambers were ineffective as recipient sites, the most superficial dermal implantation proved successful for heterotopic transplantation of single scalp hair follicle grafts, enabling hair growth during successive cycles.

Results: The study confirms the known reduction in daily hair growth rates while maintaining hair diameter. Notably, a unique and exceptional “non-correlation” was observed between scalp hair diameter and linear growth rates. While the initial shortening of the hair cycle duration was recorded in the first 3 years post-grafting, a further reduction eventually led to a “dormancy” phase in the long term (16 years post-grafting). Pharmacodynamics revealed that reactivation of hair production, following less than 3 months of topical application of a 5% minoxidil solution, suggested very slow daily growth rates and a substantial reduction in hair diameter.

Conclusion: The initial findings suggest that non-invasive methods can be used for real-time structural-functional observation of scalp hair roots, enabling the study of cellular activity and movement during successive phases of



© The Author(s) 2025. **Open Access** This article is licensed under a Creative Commons Attribution 4.0 International License (<https://creativecommons.org/licenses/by/4.0/>), which permits unrestricted use, sharing, adaptation, distribution and reproduction in any medium or format, for any purpose, even commercially, as long as you give appropriate credit to the original author(s) and the source, provide a link to the Creative Commons license, and indicate if changes were made.



the hair cycle, including aging and drug effects.

Keywords: Isolated hair follicle, live observation of hair roots, hair cycle, hair growth, confocal microscopy, *in vivo* studies, trichoscopy, phototrichogram

INTRODUCTION

In the field of human scalp hair transplantation, a few studies have explored the dynamics of hair cycles using autologous heterotopic scalp grafts (from the forearm^[1], forehead and leg^[2]). These studies have shown that heterotopic grafting temporarily affects hair growth rates for up to 3 years (in contrast to scalp-to-scalp transplantations), while re-implantation of heterotopic grafts into scalp sites restores normal growth rates^[2,3].

The surface view of the human scalp, aided by special lighting and magnification, has significantly improved in recent years. However, during extensive studies on global and dynamic imaging using contrast-enhanced phototrichogram with exogen collection (further CE-PTG-EC)^[4,5], we realized that some essential features, such as the long-term dynamics of hair cycles and the deeper micro-anatomy of the scalp follicle *in situ*, remain hidden when observing only the scalp from the surface.

To investigate the required steps for visualizing changes in deeper follicular structures throughout the hair cycle, we report here the first experiments on autologous heterotopic scalp hair follicle transplants in most superficial skin locations (i.e., parallel to the skin surface). Preliminary observations on the first cycle were briefly described in an earlier report^[6], and in this study, we expand on the dynamics of subsequent cycles observed over a 20-year period.

Besides fluctuations in hair cycles and productivity, scalp grafts entered a dormancy phase lasting several years. Reactivation, induced by the daily topical application of a Minoxidil solution (5%), resulted in the production of thinner and slow-growing hair fibers within less than 3 months.

METHODS

Experimental protocol, volunteer and ethical approval

The experimental protocol was discussed internally in April 2005. As no apparent therapeutic benefit was expected, only a single volunteer (the investigator himself) would participate in the study. The Independent Committee for Medical Ethics granted its agreement to the volunteer in writing in September 2005, as well as to all technicians and laboratories involved in the process (File data; fax dated September 15, 2005, from Chairman of Ethics Committee-RHMS-Tournai; No. 1-53306-51-580). All were duly informed about the technical details and limitations, including a tentative attempt at transfection. Following this, the volunteer gave oral consent to participate in the study.

The impact of most superficial implantation was assessed during the first two cycle phases. Once the grafts entered a sufficiently prolonged dormancy phase (no hair production for at least 96 weeks), a pharmacodynamic trial was conducted to evaluate the response of the grafted follicles to minoxidil.

This hypothesis was based on the known boosting effect of topical minoxidil application [5% solution 1X/day; Minoxidil Topical Solution further (MTS)] on the volunteer's scalp. Scalp hair regression was documented before oral treatment. Growth was stabilized with oral finasteride over a number of years^[7,8]. The maintained scalp hair follicles even further improved their productivity with the topical

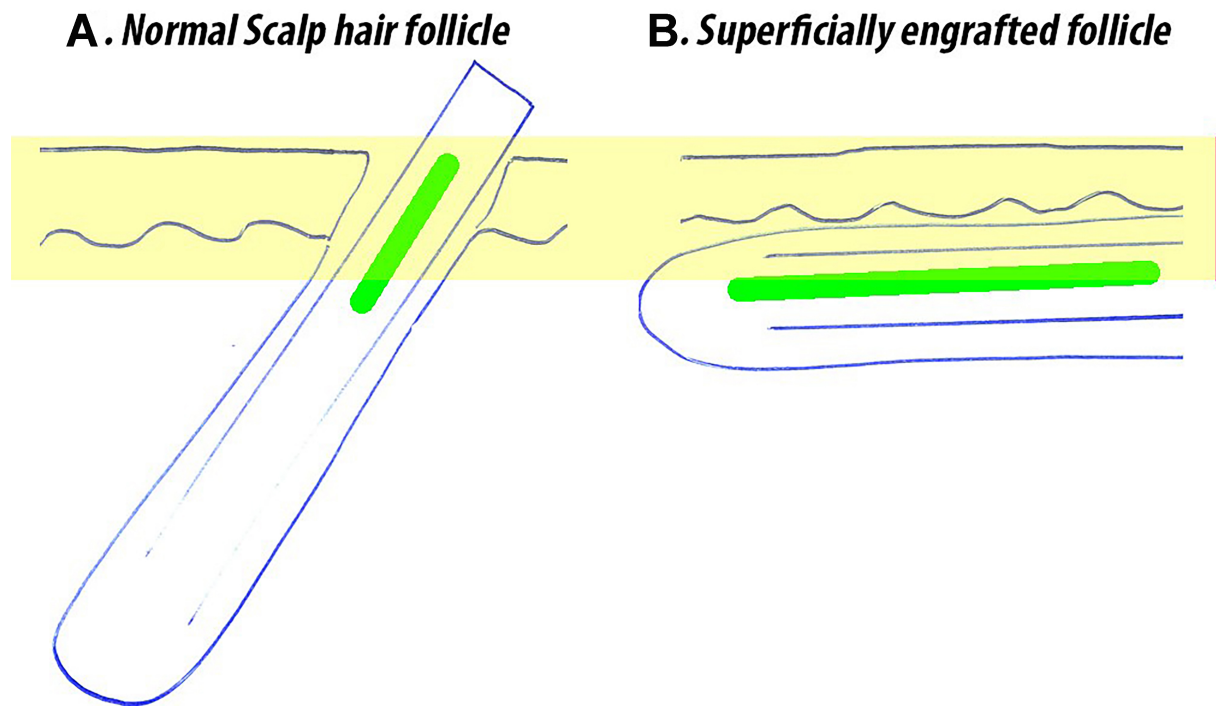


Figure 1. Rationale for most superficial dermal implantation of scalp hair follicle. In its natural implantation [(A); schematic view], surface imaging methods only access the uppermost part of the hair follicle (highlighted in yellow). Upper dermal implantation (B) theoretically enables the visualization of the entire follicle. Given the limited depth of focus of non-invasive imaging methods, i.e., 150-250 μm , our experimental study makes sense. More details on the success and failures of the experimental implantation are detailed in [Supplementary File 1](#).

administration of MTS (personal unpublished data).

Donor scalp hair follicle harvesting

Samples were collected from the typical donor site [the lower occipital region; local anesthesia (intra-dermal injection of 2% lidocaine)]. Follicular unit micro-dissection of 2 mm diameter scalp biopsies generated perfectly isolated individual scalp hair follicles ($n = 10$).

Recipient site selection and preparation

The superficial implantation [concept shown in [Figure 1](#)] required several attempts, including an unsuccessful LASER-assisted transfection experiment [see [Supplementary File 1](#) for details]. After marking the skin surface with marker dots, a small red tattoo was applied near the hair follicle opening for long-term identification.

Surface imaging of grafted sites

Repeated surface imaging was conducted using DermLite [lens equipped with light emitting diodes (LED) 3GEN™, USA] to detect hair fibers. The in-house method known as CE-PTG-EC (as described in greater detail elsewhere^[4-9], and further PTG) underwent specific adaptations during this experiment.

To clarify these adaptations, here are some practical examples:

- The harvested and implanted fibers were normally pigmented, providing excellent contrast between hair and skin. Therefore, contrast enhancement with hair dyes was not systematically applied.

- The exogen hair collection procedure was not performed immediately after implantation, but only after proper graft fixation, i.e., 10 days post-implantation.
- Similarly, the exogen hair collection step was usually skipped, as it might inappropriately and prematurely remove long hair fibers captured during the polymerization process. Notably, longer hair inside the polymerized silicone required stronger extraction forces during fiber collection^[9].

By design, it was essential to distinguish between elongation (representing shaft movement without growth, i.e., passive migration after implantation) and active growth (i.e., anagen hair production). The classical PTG involved double imaging sessions, ideally starting with short stubbles after clipping and maintaining the usual 48-h interval between images, but this interval was not always adhered to.

In May 2024, we observed that no hair had been produced by the two grafts for 96 weeks. Imaging sessions (totaling 110 images over 4 months) began at baseline (before the topical treatment) and continued through August 2024. During the treatment period, a 5% minoxidil solution was applied daily (at least twice, 0.5 mL/day; 165 applications in total; Minoxidil Biorga™). The goal was to monitor the transition from dormancy to early anagen hair production. In August 2024, hair was plucked out to validate surface measures through microscopy.

Dermal exploration with ultrasound

Post-operative dermal positioning was checked with ultrasound (Dermscan; Cortex Technology 3D-50 MHz device with high resolution). The depth of penetration was adequate, and the resolution of echograph images was sufficiently high (e.g., 3 mm^[10]) based on the present implantation methodology (less than 1 mm depth).

Dermal exploration with confocal microscopy

The procedures for *in vivo* confocal microscopy are detailed in [Supplementary File 2](#). An LSM 510 META - Zeiss Microscope [Laser: Chameleon tuneable mode-locked Titanium:sapphire laser, 90 MHz (Coherent, Santa Clara, USA), with a pulse duration of 170 fs] was employed^[11-13] (Fraunhofer Institute, Saint-Ingbert, France).

The volunteer positioned his forearm and maintained this position without further movement under the control of laboratory assistants with light microscopy.

Statistics

Descriptive statistics for repeated measurements of initial growth from grafts were provided (average \pm standard deviation). Due to the limited sample size (1 volunteer and 2 isolated scalp hair follicles), statistical testing was not performed. However, the descriptive statistics of the growth and diameter of the two regrowing “Minoxidil hair” were compared with data from 2 previous *in vivo* and *in situ* assay on Male Pattern Hair Loss^[2,14], mainly for illustrative purposes.

RESULTS

Experimental protocol, volunteer and surface imaging of grafted sites

The efficiency of implantation is important to prevent the wastage of time and effort by other investigators. Details are given in [Supplementary File 1](#).

For superficial dermal implantation, two scalp follicles yielded valuable data regarding the first two cycles (the first 4 years).

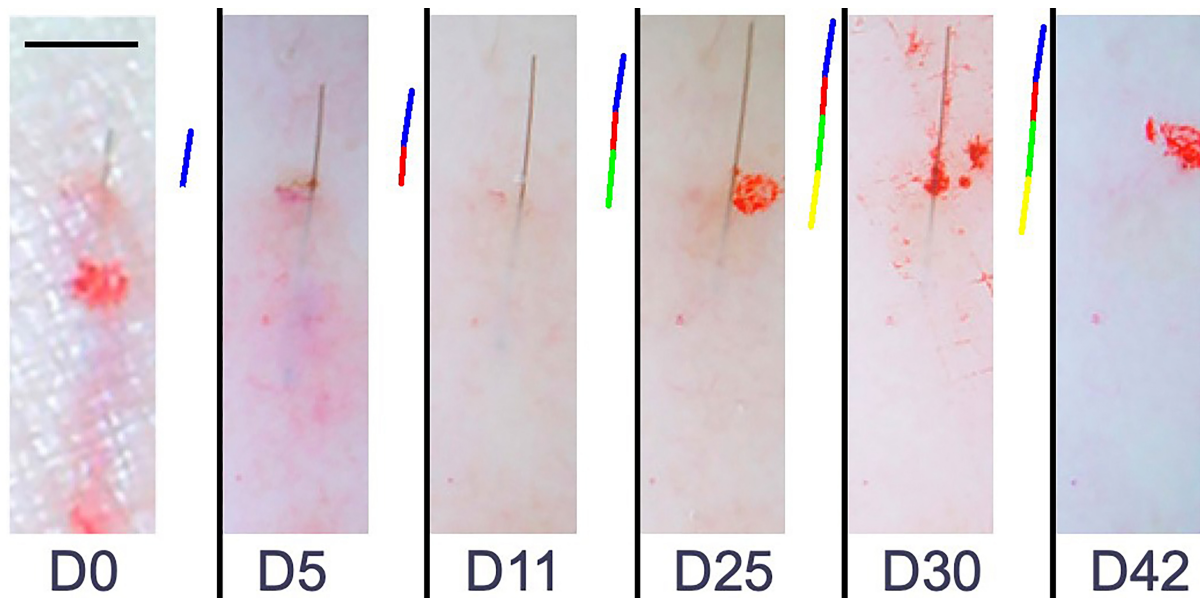


Figure 2. Short-term monitoring and hair shedding after scalp grafting. Imaging began immediately after engrafting the single hair-bearing follicle (scale bar = 1 mm; upper left corner). A red skin marker facilitated consistent imaging from D5 to D42. The proximal end of the hair shaft was highlighted each day (indicated by colored bars on the right margin of each panel). The hair fiber in the grafted follicle is represented by a blue bar (on the right side of the hair on D0). This segment shifts as it is pushed out from the graft, from D5 to D11 and from D11 to D25, respectively, indicated by additional green and yellow bars. After D25, migration ceased (indicated by the unmodified total length of the colored bars), until the hair was shed and collected on D42 [more details in [Figure 3](#)]. D: Day.

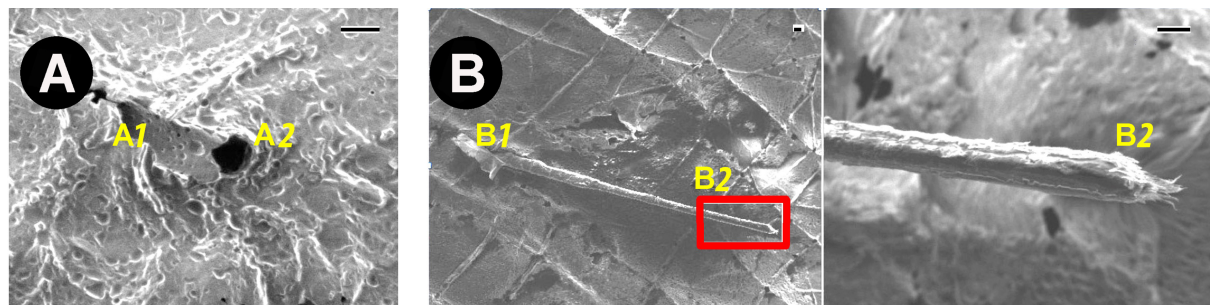


Figure 3. Exogen hair collection. Skin replicas were employed to observe the skin surface and monitor hair shafts with SEM (Scale bar = 50 μ m, the upper right corner of A and B1-B2). The use of replica material is part of the exogen collection procedure and was employed only after the graft had firmly taken, beginning on D11. (A) shows the replica on D11, highlighting the skin surface microrelief. No hair fiber is present; instead, the typical surface of the hair shaft is visible (A1) above the exit point of the grafted follicle (dark spot, A2). This demonstrates that the hair shaft was securely anchored inside the grafted follicle; (B) shows the replica on D42, where the exogen hair shaft is now entrapped in the polymerized matrix. The shaft is visible from its exit point at the skin surface (B1) down to the root end (B2). The area outlined in red is further magnified in B2 (extreme right). The shape of the “normal” cortical cells is a result of sudden anagen arrest, followed by migration (without growth) until all intercellular junctions have been dissolved, i.e., no typical telogen clubbing. SEM: Scanning electron microscopy.

Typically, during the immediate post-grafting period, repeated imaging enables clear documentation of shifts in the pre-existing hair shafts. Apparent gradual elongation of the visible part of the hair fiber results from migration after the post-implantation arrest of cell proliferation and differentiation. Intra-follicular tension, along with the natural elasticity inside the follicle, pushed the pre-existing shaft toward the skin surface, leading to shedding. This process occurred between 30 and 58 days, ending with hair shaft collection [[Figures 2 and 3](#)].

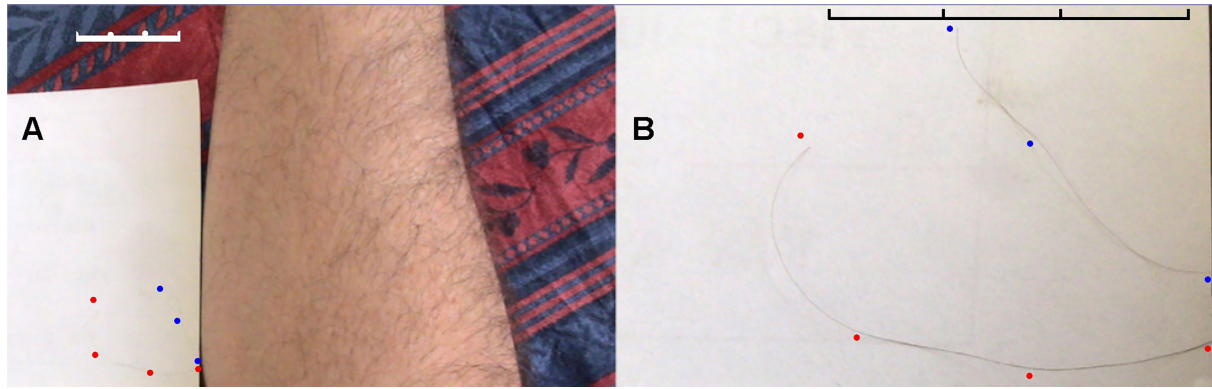


Figure 4. Long-term monitoring of the first hair cycle. Repeated imaging of hair production by the grafts reveals the length achieved during the first cycle, i.e., at 18 months post-grafting [3 cm rulers; white in (A) and black in (B)]. Both the forearm and hair are shown (A), with a higher magnification view in (B). Four red dots indicate the hair produced by the proximal graft, while three blue dots point to the barely visible hair produced by the distal graft. The total visible length of the scalp hair shafts remains significantly below the expected 18 cm fibers that would typically grow in 18 months from donor scalp follicles *in situ*.

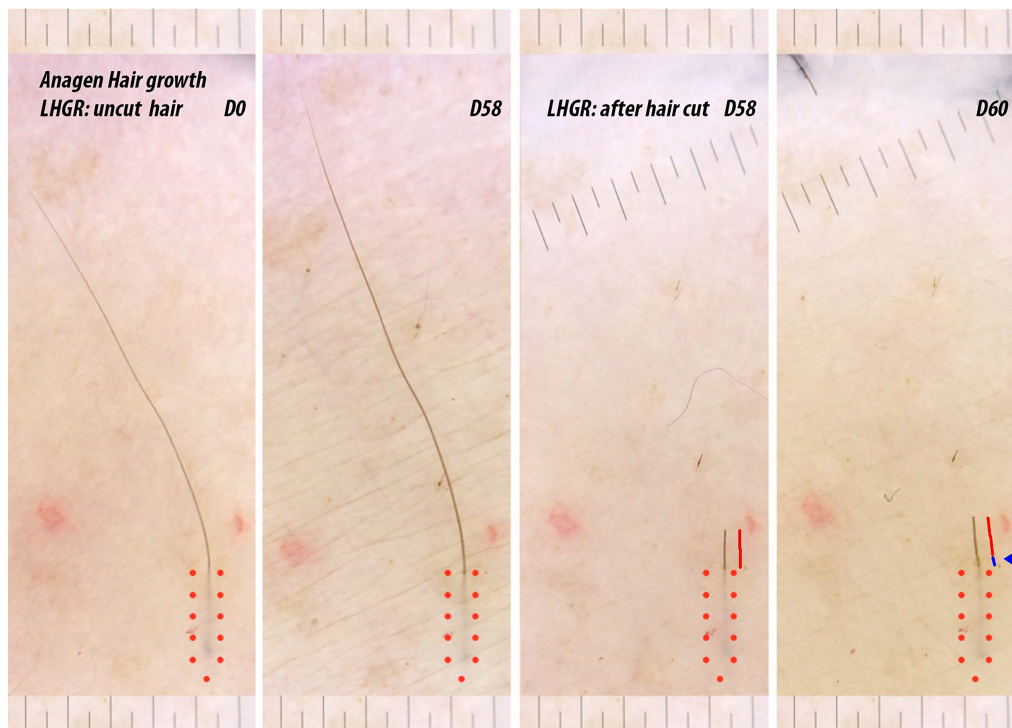


Figure 5. Hair during the second cycle and root view of implanted scalp hair follicles. During the second hair cycle, regrown hair is shown before clipping (uncut panels on the left; D0 and D58), and after clipping (panels on the right: D58 and D60). The scale bar is shown at the top and bottom of the figure (spacing: 500 μm). Hair length increases during the D0-D58 interval, but the tips of non-dyed hair vs. dyed hair (D0 vs. D58) complicate precise LHGR. However, the combination of hair dye, clipping, and repeated imaging 48 h later (on D58 and D60; panels on the right) facilitates precise growth measurement. The latter is highlighted by the short blue segment in front of the arrowhead (panel D60) and the increased length is approximately 250 μm over 48 h, corresponding to a daily growth rate of 125 μm . Direct visualization of the anagen root, with its natural pigmentation, and the ghost image of the dermal papilla are marked with 11 red dots and align with our experimental design [schematic in Figure 1; green bar in Supplementary File 1]. D: Day; LHGR: linear hair growth rate measurements.

The first anagen phase of the hair cycle was evaluated at 18 months, at which point the total length of the shafts was reduced to 4 and 6 cm [Figure 4]. The first cycle ended shortly after transitioning into the telogen

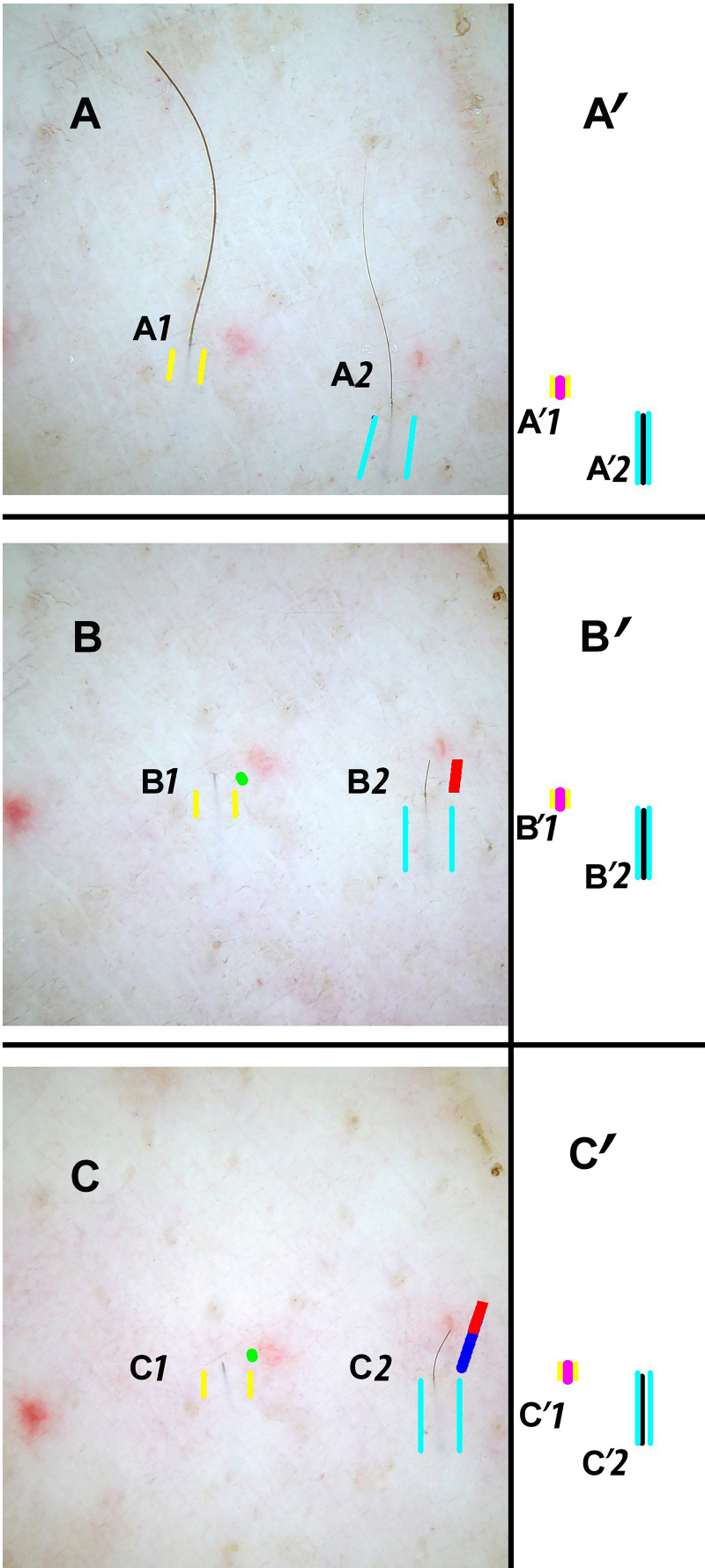


Figure 6. Root visibility depends on the depth of implantation and pigment production during the anagen stage of the hair cycle. The panels on the left (A, B, C) display the surface view of the grafts and hair, while the panels on the right (A', B', and C') are schematic drawings of the visible dermal aspects of the same samples. The spontaneous - non-synchronized - cycling is reflected in the hair production from two grafted scalp follicles after hair dying, before clipping (A), immediately after clipping (B), and 48 h later (C). In the original surface views (panels on the left), attention is drawn to the visible root segments (in the middle of two yellow bars for the proximal graft and two turquoise bars for the distal graft). The unclipped, relatively long hair from the proximal grafted follicle is shown on the extreme left (A and A1). This follicle has recently entered the resting (telogen) phase after terminating its growth (anagen), as demonstrated by repeated clipping and imaging. There is "no elongation" of the clipped hair fiber (as indicated by the green dot in b1 and c1, respectively). The surface imaging cannot capture the deeper root of the proximal graft [the magenta bar between the two parallel yellow bars in A', B' and C' highlights intra-epidermal segments A'1, B'1 and C'1 (length $\pm 100 \mu\text{m}$)]. The follicle on the right side (A2 in A; distal graft) displays a tapered, less pigmented tip. After hair dying, the tip appears as a recently regrown, thin fiber. The root length is roughly displayed (seen in A2, B2, and C2, and schematically in A'2, B'2, and C'2; marked by a black vertical line between two magenta bars [estimated depth inside the follicle: 300 to 500 μm]). The stubble remaining after clipping (B2; red bar) significantly elongates, reflecting hair growth as seen in image C2, which was captured 48h after the image in B2, and the added blue proximal segment demonstrates the production of anagen hair (with an estimated linear growth rate of 120 $\mu\text{m}/\text{day}$).

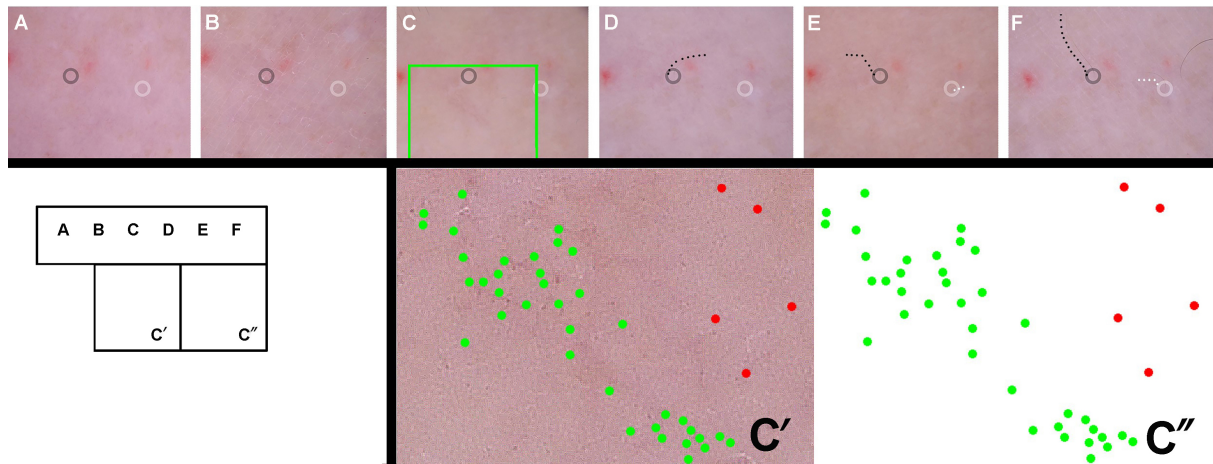


Figure 7. Transition from dormant stage (no hair production for 3 years) to anagen stage induction by minoxidil topical solution. After a prolonged dormant phase characterized by no hair production over 36 months, we successfully induced regrowth in both grafts through the topical application of a 5% MTS. Imaging was conducted biweekly, starting from May 2024 (A shows the baseline image before application, and panel F shows the final result). MTS 5% was applied at least twice daily, with a light massage in the targeted area. Hair shafts emerged from the follicular ostia (proximal graft indicated by the grey circle on the left and distal graft by the white circle on the right), initially as fine, poorly pigmented fibers. Over time, between D45 (D) and D60 (E) post-treatment, more and more pigmented and curved hairs were observed. Interestingly, around D30 of MTS application, before the shafts appeared at the skin surface, a disappearing reticular pattern of capillary blood vessels was seen along the path that would later be followed by the regrowing root (proximal graft). Computer-assisted image analysis of panel "C" identified a number of clusters. Clusters containing at least three pixels were dot-mapped. Based on their proximity to the implanted graft, the dots were color-coded (green for the graft area and red for more distant dermal regions). As illustrated in C' and C'', 36 dots were located in the root area and 5 in more remote dermal fields. The latter were considered background noise, as opposed to the signal density associated with the induced regrowing root. Growth was maintained with MTS until August 2024 (F). MTS: Minoxidil lotion.

and shedding phase (no growth for 3 months).

Interestingly, although it was already visible during the first cycle, trans-illumination with dermoscopy enabled direct visualization of the anagen root with the natural pigmentation of the shaft [second cycle shown in Figure 5]. The root also forms a cup shape that indirectly points to the hair bulb and its dermal papilla. These features faded during the telogen phase at the end of the second cycle and reappeared only in the later cycle in the most superficially implanted graft [Figure 6]. All dermoscopic images captured the deepest intra-follicular elements since the grafts were located very superficially and remained visible as long as pigment provided sufficient contrast. The estimated duration of the first two cycles ranged from 24 to 20 months.

Throughout this initial period, the diameter remained within the range of the donor scalp hair (mean \pm standard deviation: $62 \pm 22.26 \mu\text{m}$). However, hair growth rates eventually dropped below the threshold of $150 \mu\text{m}/\text{day}$, which is the limit used in our laboratory to distinguish between growing and non-growing hair, i.e., to differentiate between the anagen or “catagen - telogen” phases [Figure 7].

With precise time control, growth rates of the scalp grafts were measured after clipping and repeated imaging. These growth rates decreased compared to the linear hair growth rate measurements (LHGR) measured *in situ* (cycles 1 and 2, 4 years; average daily growth rate \pm standard deviation of 15 measurements: $161 \pm 32 \mu\text{m}/\text{day}$ vs. normal growth rates: $379 \pm 49 \mu\text{m}/\text{day}$ ^[4]). The diameter during this period remained within the range of the donor scalp hair (mean \pm standard deviation: $62 \pm 22.26 \mu\text{m}$) [Figures 8 and 9].

Dermal exploration with ultrasound

Ultrasound imaging allows for the visualization of the implantation level and the insertion of the hair follicle beneath the intact epidermis, except at the point where the hair emerges. The imaging captures the longitudinal structure of the hair follicle in a single plane [Figure 10]. Hair roots were located in a moderately hypo-echogenic dermal area (unexposed to sunlight; 55-year-old male) and remained in the most superficial dermis (not deeper than 2 mm from the epidermis).

Dermal exploration with confocal microscopy

Details of *in vivo* confocal microscopy are illustrated in Supplementary File 2. A series of images is provided, showing two hair grafts [Figure 11]. The hair shaft produced during the first cycle anagen phase post-grafting (November 2005) serves as a reference to trace the hair follicles down to $120 \mu\text{m}$ inside the hair follicle [along the green line shown in Figure 1]. This is approximately the limit of signal detection with confocal microscopy along the vertical axis (about $200\text{--}250 \mu\text{m}$ from the skin surface). It is evident that the ideal geometry, as outlined in Figure 1, was not achieved during the actual procedure. Given the implantation angle, *in vivo* observation extended to the hair bulb and dermal papilla. While confocal microscopy achieved promising depths - estimated at $500 \mu\text{m}$, roughly twice the depth reached through direct observation on the scalp, our transfection experiment failed. As a result, the pigment in the anagen hair shaft and its autofluorescence were the only guide for investigators during this experimental stage.

DISCUSSION

Graft take and 1st-2nd cycles

No graft take was observed after intra-epidermal implantation. All grafts were rapidly eliminated and we presume that rapid epidermal healing prevented essential vascular events to support follicular recovery^[15,16].

The duration of graft take aligns with Nordström’s proposal of 8 days^[1], as dermal implants clearly resisted our exogen extraction procedure^[9]. While shedding is a trivial observation, we disagree with Kim *et al.*’s hypothesis, which suggests that post-grafting shedding occurs as early as 2 weeks after undergoing the “catagen and telogen” phases^[2]. We were unable to observe the normal end-stage completion of the natural cycle, even though the interval before shedding was longer. The images of the root end released upon post-operative shedding seemed to reflect an abrupt arrest in anagen, rather than a typical shedding process.

New cycles are spontaneously initiated in most heterotopic transplantation experiments, regardless of the depth or angle of dermal implantation. Nordström considered that hair loss from grafts taken from balding sites and transplanted to the forearm was consistent with spontaneous loss from the original balding donor sites, and Hwang *et al.* reported a 60% survival rate of non-balding grafts after 3 years^[1,3]. Based on our

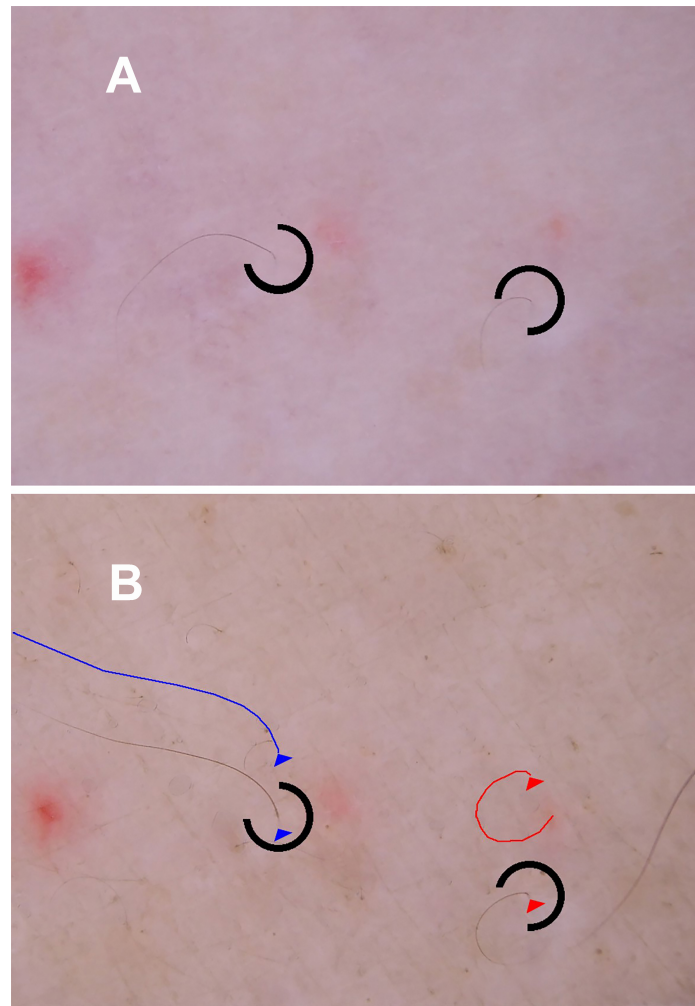


Figure 8. Reactivation of miniaturizing follicles and slow growth with minoxidil 5%: The role of hair dye for improved imaging. Panels a and b show surface views of the engrafted hair follicles: without a hair dye (A) and after dye (B). The tattoo on the left (closer to the elbow) relates to “no hair growth” after LASER-attempt of transfection. The two hair-producing follicles are highlighted by rings. The ring in the center opens upward, drawing attention to the exit point of a longer hair in the proximal graft, while the ring opening downward points to a shorter hair in the distal follicle. A hair dye session on August 9, 2024, underpinned again the benefits of Contrast-Enhancement procedure: the very fine, barely visible tips of the hairs in panel a are much more clearly visible after hair dyeing (B). The improved visibility of the hair length and diameter in panel b further details the exit points from the grafted follicles (blue or red triangles) and hair length (blue or red curved lines along the hair fibers). Diameter and length estimates were confirmed through light microscopy on plucked fibers. Daily growth rates of 116 and 87 μm were recorded for the proximal and distal grafts, respectively, based on measurements of two plucked, un-clipped hairs.

longer-term graft monitoring, we speculate that surface observation of a proportion of follicles rapidly entering dormancy may have been misinterpreted by previous authors as “failures in terms of hair follicle survival”. Indeed, follicle-bearing grafts with slowing growth rates returned to normal growth rates when grafted back into their original physiological sites^[2,3]. This clearly suggests the reversibility of some functional defects, e.g., growth rate abnormalities. Consequently, it remains difficult to definitely distinguish between irreversible structural deficiencies and transient functional changes.

Regarding hair cycles, to the best of our knowledge, there is little or no information available on autologous heterotopic grafting. In this experiment, we observed hair production of 4 and 6 cm, rather than the expected 12-18 cm^[4,14], consistent with findings from other authors.

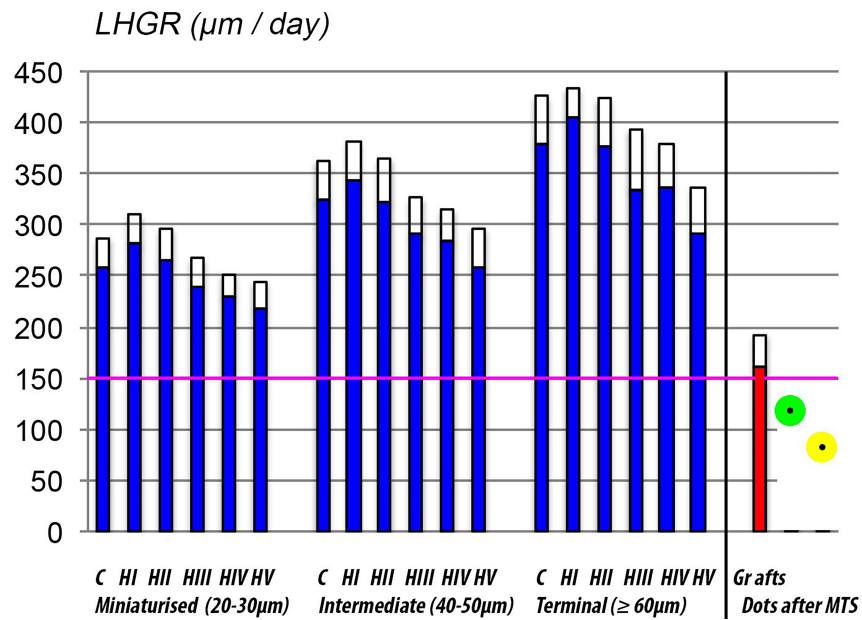


Figure 9. Statistics of linear growth rates *in vivo* and *in situ* and after grafting. This graph presents statistics on linear hair growth rates [Y-axis: LHGR µm/day; averages with standard deviation (blue and empty bars, respectively)] from a previously published study involving male participants [90 PTGs from healthy controls (C) and 110 from subjects affected with patterned hair loss (Hamilton classification with severity grades I to V; HI to HV^[4])]. The hair diameters (categorized on the X-axis as 20-30 µm, 40-50 µm, and ≥ 60 µm, respectively, for miniaturized, intermediate, and terminal) clearly influence LHGR according to clinical status (control vs. patients). *In vivo* and *in situ* LHGR are shown in comparison with average growth rates from grafted follicles before MTS treatment [grafts; red bar; an average of 17 data points with standard deviation (empty bar)]. Taking hair diameter into account, the growth rates of reactivated grafts (represented by green and yellow dots after MTS, respectively, for proximal and distal grafts at the extreme right of the bar graph) barely reached 50% of the initial growth rates. In any case, LHGR were lower than the *in vivo* recorded growth rates observed in the thinnest scalp hair *in situ*^[4,14]. MTS: Minoxidil lotion; LHGR: linear hair growth rate measurements; PTGs: phototrichogram.

Using surface imaging on clipped hair, we observed rather stable diameters in the first successive fibers until the follicles eventually entered a non-productive stage, also known as the apparent “dormancy” stage.

Longer-term cycling and dormancy

Previous studies on heterotopic grafts of scalp hair follicles typically ended after 3 years of observation^[1,3], a time frame probably too short to fully document the dormancy stage (especially in cases of balding scalp transplantation^[1]).

In the present experimental setup, we exploited a situation that would be considered as “not appropriate” in transplantation clinics. The “see-through effect”^[17] seems to be a critical initial step in performing most superficial grafting in view of a long-term follow-up.

The last phase of our study involved documenting a 3-year period during which no hair production occurred. We decided to exploit this unique opportunity to test the effect of topically applied minoxidil. Clinical trials^[18] suggest that regrowth can be expected within 6-8 weeks, peaking at 12-16 weeks. Our more recent study^[19], which combined minoxidil and finasteride, indicated that all initiated anagen hair follicles were significantly activated by 2 months, reaching a peak at 3 months, while exogen collection was statistically significantly reduced at the 2-month mark.

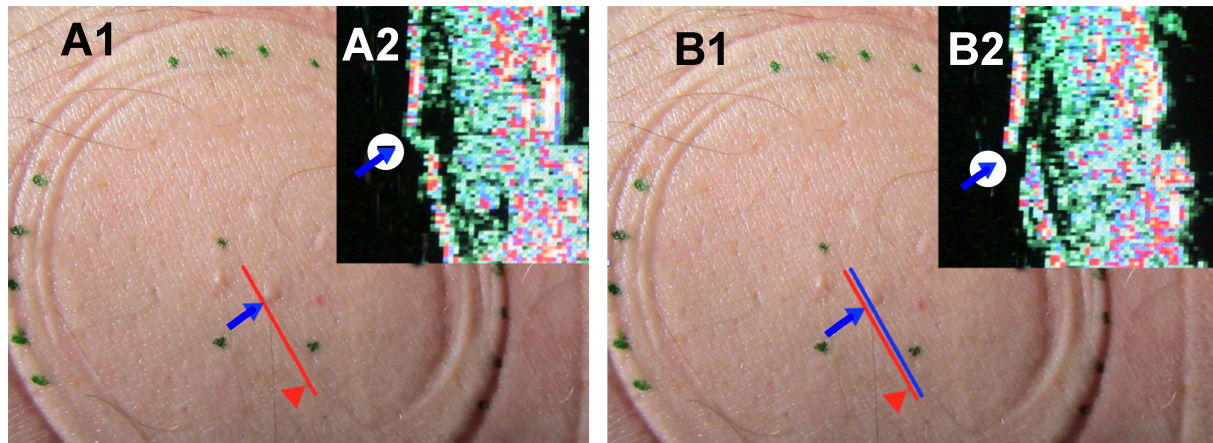


Figure 10. Ultrasound study of follicular implantation. For clinical illustration, two hair fibers were gently pulled to elevate the skin-hair junction at the exit point. The region of interest was then marked with three green dots, and the margins of the circular probe were outlined with 13 green dots. These steps help position the ultrasound probe to focus on the opening of the grafted hair follicle to be scanned (indicated by red and blue lines). Once in place, the scanning allows beamer steps in the order of 100 μm shifts. In A1, the blue arrow points to the opening of the grafted hair follicle, where the hair shaft exits at the skin surface. The red line indicates the path of the scanning beam, and the resulting ultrasound image is shown in panel A2. The image clearly shows the epidermis as continuous (blue arrow with an arrowhead on the white spot in the upper right corner of panel A2), with a slight epidermal bump and a hypo-echogenic field beneath. In panel B1, the blue line illustrates the axis of a shifted beam (at a 200 μm distance to the right side of the red axis shown in A1). The corresponding ultrasound image (B2) clearly shows a disruption in the epidermis (blue arrow with an arrowhead on the white spot in the upper right corner of B2). The follicle remains in continuity with the hypo-echogenic zone underneath, at an estimated average depth of 250 μm beneath the epidermal surface, while the fiber inside the follicle appears echogenic. The skin below the arrow shows a hypo-echogenic dermis, which may partly, though not exclusively, indicate superficial dermal atrophy due to aging (or photo-aging, although the volar aspect of the forearm was less sun-exposed).

The grafted dormant follicles responded rapidly, with a transient stage of vascular network formation around the follicular trail (between weeks 3 and 5). This was followed by the appearance of a barely visible tip (with low pigment loading) at weeks 5-6. Finally, regrowth of intermediate or thin hair at very slow rates concluded the observation period of MTS application (2.5 months).

In conclusion, several hypotheses have been discussed regarding the survival, performance, and cycle of displaced scalp hair follicles. We acknowledge that a potential undesired effect of classical transplantation (i.e., the see-through effect) has been repurposed into an efficient solution for running basic experiments.

Clearly, future work will be required to encompass all dimensions, both strengths and weaknesses, of this method.

Some notable strengths include the live observation of human scalp hair bulbs, the ability to repeat complete hair cycles *in vivo*, the identification of a real dormancy stage, and proof of rapid regrowth induced by the topical application of a hair-growth-promoting drug.

On the other hand, weaker aspects include the uncertainties and potential confounding factors related to the lifespan of human volunteers, reduced growth rates, the long duration inherent to scalp hair studies, and possible aging-related changes.

In addition to speculations about the precise *in situ* identification of hair cycle stages and the influence of hair root characteristics on follicle performance *in vitro*^[20,21], we acknowledge the limitations and uncertainties surrounding experimental models, including the grafting of scalp hair follicles onto rodents

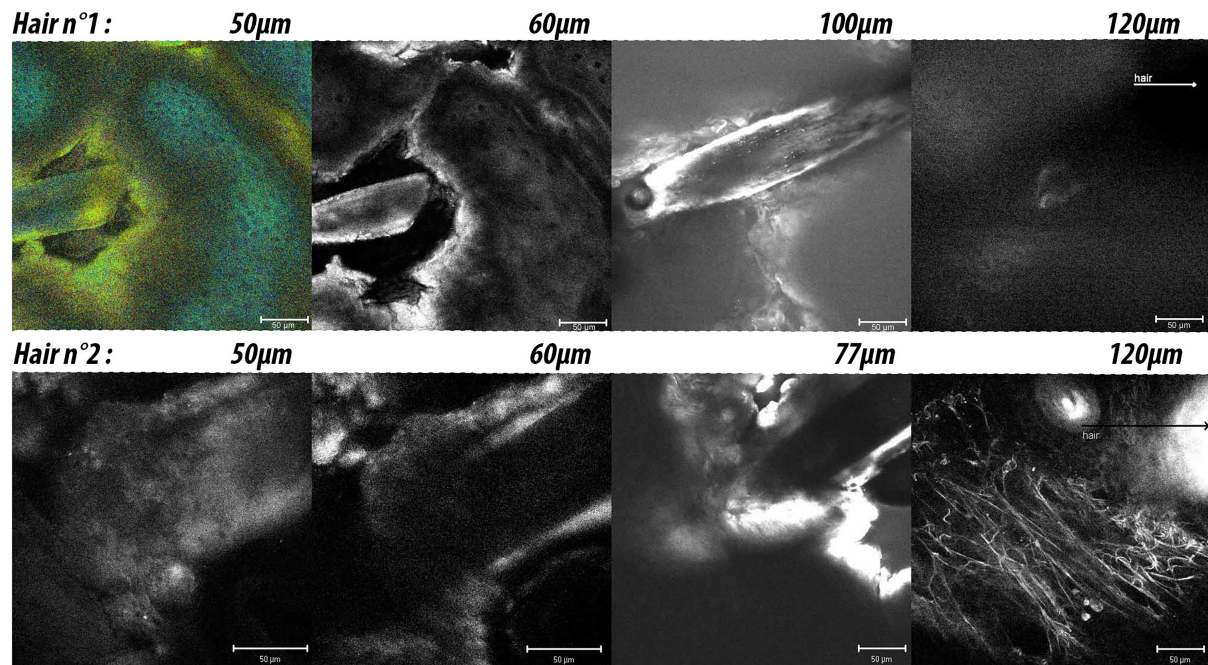


Figure 11. Dual confocal microscopy of implanted scalp hair follicles. Follicles 1 and 2 (proximal and distal) were imaged 1 month after the initiation of visible anagen hair at the skin surface (i.e., 3 months after implantation). At intra-follicular depths ranging from 50 to 120 μm , we reached the detection threshold for auto-fluorescence of hair shafts. The top panels show images of hair inside follicle 1 and the bottom panels for hair follicle 2. The top-left panel of Hair 1 (at an intra-follicular depth of 50 μm) displays a fluorescence lifetime image that distinguishes different components based on the lifetime of their fluorophores. Living cells are typically artificially colored blue [NAD(P)H/NADH] and keratin in green/yellow. Deeper within the follicle, the only image is a blurred ring (top panel: hair 1 at an intra-follicular depth of 120 μm), while images from hair 2, taken at a similar intra-follicular depth (bottom panel: hair 2 at 120 μm), show epithelial cells (infundibulum or outer root sheath) along with a fine network of collagen fibers, reflecting the perifollicular dermal sheaths or superficial dermal structures.

and humans. Such a topic has been discussed in some detail recently^[22]. We refer interested readers to discussions on the biological considerations and validity of experimental models, as well as their clinical relevance (e.g., genetic conditions, modulation of phenotype such as aging, miniaturization, follow-up duration^[23,24], etc.). Drawing from previous experimental data from our laboratory, we will tentatively suggest some ideas for future research in [Supplementary File 2](#).

Nevertheless, we are deeply convinced that this model could represent a significant advancement, providing a more efficient way to apprehend cellular interactions within living hair follicles, compared to short-term *ex vivo* or *in vitro* survival studies. Unlike *in vivo* studies^[23,24], there have been no reports on complete hair cycles of isolated hair follicles *in vitro*^[21]. To us, it is obvious that isolated follicles constantly, irreversibly, and rather rapidly regress with declining growth rates, ultimately leading to follicular death after a very short term.

DECLARATIONS

Acknowledgments

The image of the first cycle was reprocessed from the Belgian dermatology journal “Skin 2010”, with permission granted by Dr. V. Leclercq (Editor) to reprocess [Figure 6] published therein^[6]. The author greatly appreciates the assistance of Mrs. Iris Riemann (Fraunhofer, Sankt-Ingbert, France) during the confocal imaging procedures, as well as her help in getting permission to publish the images and accompanying comments. Additionally, the author appreciates the encouraging support from Fraunhofer

EUROPE (Brussels Office, Mrs. Verena Fennemann). Scanning Electron Microscopy images were generated in collaboration with Materia Nova (University of Mons, Belgium). The author is grateful for the technical assistance of Mrs. Véronique Ronsse, whose dedication during sustained imaging sessions over the last 20 years has been invaluable to this long-term project. The author also expresses sincere gratitude to Mr. Charles Cassells, Mrs. Oonagh Duckworth, and Prof. David Hugh Rushton for their proofreading of this manuscript.

Authors' contributions

The author contributed solely to the article.

Availability of data and materials

Not applicable.

Financial support and sponsorship

None.

Conflicts of interest

The author declared that there are no conflicts of interest.

Ethical approval and consent to participate

Research involving human subjects, human material or human data was performed in accordance with the Declaration of Helsinki and approved by the Independent Committee for Medical Ethics in September 2005.

Consent for publication

Not applicable.

Copyright

© The Author(s) 2025.

REFERENCES

1. Nordström REA. Synchronous balding of scalp and hair-bearing grafts of scalp transplanted to the skin of the arm in male pattern baldness. *Acta Derm Venereol.* 1978;59:266-7. Available from: <https://medicaljournalssweden.se/actadv/article/view/17137/20989>. [Last accessed on 24 Feb 2025].
2. Kim JC, Kim MK, Choi YC. Regeneration of the human scalp hair follicle after horizontal sectioning: implications for pluripotent stem cells and melanocyte reservoir. In: Van Neste DJJ, Randall V, Baden H, Ogawa H, Oliver R, Editors. Hair research for the next millennium. Elsevier; 1996. pp. 135-9. Available from: https://scholar.google.com/scholar?cluster=1427582052650609232&hl=zh-CN&as_sdt=0,48. [Last accessed on 28 Feb 2025].
3. Hwang S, Kim JC, Ryu HS, et al. Does the recipient site influence the hair growth characteristics in hair transplantation? *Dermatol Surg.* 2002;28:795-9. DOI PubMed
4. Van Neste D. Exhaustive analysis of scalp hair regression: subjective and objective perception from initial hair loss to severe miniaturisation and drug-induced regrowth. *Plast Aesthet Res.* 2021;8:16. DOI
5. Van Neste D, Rushton DH, Westgate GE, Duteil L, Roegies K, Ronsse VV. A segmental approach to scoring hair density from global images: introducing the scalp coverage scoring method for clinical trials and practice. *Nat Cell Sci.* 2024;2:59-67. DOI
6. Van Neste D. Cinq questions sur les récentes évolutions dans le domaine des techniques d'imagerie capillaire non invasives. *Skin.* 2010;13:144-9.
7. Van Neste D. Natural scalp hair regression in preclinical stages of male androgenetic alopecia and its reversal by finasteride. *Skin Pharmacol Physiol.* 2006;19:168-76. DOI PubMed
8. Van Neste D. Maintenance of optimised hair growth from viable terminal scalp hair follicles at baseline with oral finasteride in male pattern hair loss and first evidence of a "drug dependency" and a post-finasteride "rebound effect". *Skin Res Technol.* 2019;25:712-9. DOI PubMed
9. Van Neste D, Leroy T, Conil S. Exogen hair characterization in human scalp. *Skin Res Technol.* 2007;13:436-43. DOI PubMed

10. Mlosek RK, Malinowska S. Ultrasound image of the skin, apparatus and imaging basics. *J Ultrason.* 2013;13:212-21. [DOI PubMed PMC](#)
11. Denk W, Strickler JH, Webb WW. Two-photon laser scanning fluorescence microscopy. *Science.* 1990;248:73-6. [DOI PubMed](#)
12. König K. Multiphoton microscopy in life sciences. *J Microsc.* 2000;200:83-104. [DOI PubMed](#)
13. König K, Riemann I. High-resolution multiphoton tomography of human skin with subcellular spatial resolution and picosecond time resolution. *J Biomed Opt.* 2003;8:432-9. [DOI PubMed](#)
14. Leroy T, Van Neste D. Contrast enhanced phototrichogram pinpoints scalp hair changes in androgen sensitive areas of male androgenetic alopecia. *Skin Res Technol.* 2002;8:106-11. [DOI PubMed](#)
15. Beerens EG, Slot JW, van der Leun JC. Rapid regeneration of the dermal-epidermal junction after partial separation by vacuum: an electron microscopic study. *J Invest Dermatol.* 1975;65:513-21. [DOI PubMed](#)
16. Lange-Asschenfeldt B, Alborova A, Krüger-Corcoran D, et al. Effects of a topically applied wound ointment on epidermal wound healing studied by *in vivo* fluorescence laser scanning microscopy analysis. *J Biomed Opt.* 2009;14:054001. [DOI PubMed](#)
17. Park JH, Ho YH, Manonukul K. A practical guide to hair graft placement using the sharp implanter method. *Clin Cosmet Investig Dermatol.* 2023;16:1777-85. [DOI PubMed PMC](#)
18. Messenger AG, Rundegren J. Minoxidil: mechanisms of action on hair growth. *Br J Dermatol.* 2004;150:186-94. [DOI PubMed](#)
19. Neste D. Placebo-controlled dose-effect studies with topical minoxidil 2% or 5% in male-patterned hair loss treated with oral finasteride employing an analytical and exhaustive study protocol. *Skin Res Technol.* 2020;26:542-57. [DOI PubMed PMC](#)
20. Tételin C, Van Neste D. Linear hair growth rate and diameter of hairs grown *in vitro*: a relevant correlation. In: Van Neste D, Randall V, Baden H, Ogawa H, Oliver B, Editors. Hair research for the next millenium. Elsevier Scienc, Excerpta Medica, International Congress Series 1111; 1996. pp. 183-6.
21. Jimenez F, Alam M. The proportion of catagen and telogen hair follicles in occipital scalp of male androgenetic alopecia patients: challenging the established dogma. *Exp Dermatol.* 2024;33:e70001. [DOI PubMed](#)
22. Oh JW, Kloepper J, Langan EA, et al. A guide to studying human hair follicle cycling *in vivo*. *J Invest Dermatol.* 2016;136:34-44. [DOI PubMed PMC](#)
23. Brouwer B, Tételin C, Leroy T, Bonfils A, Van Neste D. A controlled study of the effects of RU58841, a non-steroidal antiandrogen, on human hair production by balding scalp grafts maintained on testosterone-conditioned nude mice. *Br J Dermatol.* 1997;137:699-702. [PubMed](#)
24. Van Neste D, Gillespie RC, Marshall A, Taieb, De Brouwer B. Morphological and biochemical characteristics of trichothiodystrophy-variant hair are maintained after grafting of scalp specimens on to nude mice. *Br J Dermatol.* 1993;128:384-7. [DOI PubMed](#)